# Stochastic dynamics and logistic population growth

Vicenç Méndez,[1] Michael Assaf,[2] Daniel Campos,[1] and Werner Horsthemke[3]

[1]*Grup de Física Estadística, Departament de Física, Facultat de Ciències, Edifici Cc, Universitat Autònoma de Barcelona,*
*08193 Bellaterra, Barcelona, Spain*

[2]*Racah Institute of Physics, Hebrew University of Jerusalem, Jerusalem 91904, Israel*

[3]*Department of Chemistry, Southern Methodist University, Dallas, Texas 75275-0314, USA*

The Verhulst model is probably the best known macroscopic rate equation in population ecology. It depends on two parameters, the intrinsic growth rate and the carrying capacity. These parameters can be estimated for different populations and are related to the reproductive fitness and the competition for limited resources, respectively. We investigate analytically and numerically the simplest possible microscopic scenarios that give rise to the logistic equation in the deterministic mean-field limit. We provide a definition of the two parameters of the Verhulst equation in terms of microscopic parameters. In addition, we derive the conditions for extinction or persistence of the population by employing either the momentum-space spectral theory or the real-space Wentzel-Kramers-Brillouin approximation to determine the probability distribution function and the mean time to extinction of the population. Our analytical results agree well with numerical simulations.

## I. INTRODUCTION

Quantitative models of population dynamics have attracted an enormous amount of interest from biology to mathematics and physics [1–3]. In the deterministic limit, these models coincide with macroscopic rate equations based on phenomenological laws. The simplest one corresponds to the Malthus law, where the per capita rate of change in the number of individuals is constant, resulting in a linear growth rate for the population $dn/dt = rn$. The population grows exponentially $n(t) = n_0 \exp(rt)$, where $r$ is the intrinsic growth rate and $n_0$ is the initial population. Unlimited exponential growth is patently unrealistic and factors that regulate growth must be taken into account. The most famous extension of the exponential growth model is the Verhulst model, also known as the logistic model, where the per capita rate of change decreases linearly with the population size. The population's growth rate $dn/dt = rn(1 - n/K)$ is now a quadratic function of the population size, where $K$ is known as the carrying capacity. This equation was derived initially by Verhulst in 1845 [4,5] and was rediscovered later by Pearl in 1920 [6]. Other models, such as the Gompertz growth $dn/dt = \alpha n \ln(K/n)$, exhibit many of the same properties, but the logistic equation is arguably the best-known and most widely applied rate equation for population growth and population invasion [1,7].

These models are deterministic and ignore fluctuations. Real populations evolve in a stochastic manner, experiencing intrinsic noise (or internal fluctuations) caused by the discreteness of individuals and the stochastic nature of their interactions (see, e.g., [8–13]). When the typical size of the population is large, fluctuations in the observed number of individuals are typically small in the absence of external or environmental noise. The dynamics of the population then can be described by a deterministic mean-field rate equation. In the case of the logistic equation, the population evolves from an initial condition to a stable stationary state, where the population size equals the carrying capacity and persists forever. However, if the typical population size is not large,

internal fluctuations can lead to the extinction of the population [14]. The effects of internal fluctuations have been studied in predator-prey models [15,16], epidemic models [17–23], cell biology [24], and ecological systems [13]. In particular, extinction of a stochastic population [11,25,26], which is a crucial concern for population biology [27] and epidemiology [28,29], has also attracted scrutiny in cell biochemistry [30] and in physics [31,32].

To describe the intrinsic noise of populations, we adopt individual-based models, also called stochastic single patch models [33,34]. An individual-based formulation provides several advantages. It is often easier to define an ecological system in terms of the events that govern the dynamics of the system at the level of individuals. Population-level models, such as the Verhulst equation, can then be derived analytically as the mean-field approximation, instead of simply be postulated phenomenologically. In this way, individual-based models provide a microscopic basis for the usual ecological rate equations and the range validity of the latter can be established by comparing its predictions with those of the former. Individual-based models capture the fact that populations consist of discrete individuals undergoing random events corresponding to birth (reproduction of the population), competition (between individuals for limited resources), and death (natural decay of individuals). It is well known that different types of individual-based schemes are described by the same Verhulst equation in the deterministic limit. Since extinction is ultimately caused by the stochastic nature of the interactions between individuals, it is critical to analyze how the details of the individual processes affect the ultimate fate of the population or the time to extinction. We explore a variety of stochastic interactions between individuals, all of which give rise to the logistic equation in the mean-field limit. We find different dynamical behaviors, such as persistence or extinction, of a population that experiences birth, death, and competition processes. Extinction is due to rare fluctuations and the mean extinction time (MET) of the population strongly depends on the microscopic details of the processes, such as the

number of newborn individuals or the number of individuals removed due to exclusive competition. We obtain analytical solutions for the probability distribution function (PDF) of individuals, if the population persists, and for the MET, if the population becomes extinct. Our analytical results are compared with numerical simulations, performed using the first reaction method [35]. We consider the birth-and-death and birth-competition-death cases separately, making use of the momentum space spectral theory [36,37] and the real-space WKB theory [26], respectively.

## II. MASTER AND MEAN-FIELD EQUATIONS FOR GENERAL BIRTH-COMPETITION-DEATH PROCESSES

We investigate individual-based models of populations in which the following birth, competition, and death processes occur:

$$bX \xrightarrow{\lambda} (a + b)X, \tag{2.1a}$$

$$cX \xrightarrow{\mu} (c - d)X, \tag{2.1b}$$

$$X \xrightarrow{\gamma} \emptyset, \tag{2.1c}$$

where $a$, $b$, $c$, and $d$ are positive integers and $d \leqslant c$. Such processes occur also in chemically reacting systems and it is convenient to adopt the language of chemical kinetics to make a connection with the literature of stochastic chemical models. Therefore, we will often refer to the processes of (2.1) as reactions. If $d = c$, the last two reactions are death reactions, due to competition between $c$ individuals ($cX \xrightarrow{\mu} \emptyset$) or due to natural decay ($X \xrightarrow{\gamma} \emptyset$). We make the standard assumption that the reaction scheme (2.1) defines a Markovian birth-and-death process (see, e.g., [15,32,38,39]) and employ the master equation, also known as the forward Kolmogorov equation, to describe the temporal evolution of $P(n,t)$, the probability of having $n$ individuals at time $t$,

$$\frac{\partial P(n,t)}{\partial t} = \sum_r [W(n - r,r)P(n - r,t) - W(n,r)P(n,t)].$$

$$\tag{2.2}$$

Here $W(n,r)$ are the transition rates between the states with $n$ and $n + r$ individuals and $r = \{r_1, r_2, r_3\} = \{a, -d, -1\}$ are the transition increments. Equation (2.2) can generally only be solved in the stationary limit $\partial P(n,t)/\partial t = 0$ and only for the special case that $a = d = 1$, i.e., only single-step processes occur in the population. Then the condition of detailed balance holds, which significantly simplifies the theoretical analysis, and exact analytical expressions can in principle be obtained for the stationary PDF or the MET. (For recent reviews, see, for example [11,40,41].) We emphasize that we study the general generic case of arbitrary $a$ and $d$ to elucidate how the microscopic details affect the PDF or the MET. Calculating the stationary PDF or the MET is highly nontrivial for multistep reactions and this case has only recently begun to be addressed.

The transition rates corresponding to each reaction $W(n,r)$ are obtained from the reaction kinetics [32] and for (2.1) read

$$W(n,a) = \frac{\lambda}{b!} \frac{n!}{(n - b)!}, \tag{2.3a}$$

$$W(n, -d) = \frac{\mu}{c!} \frac{n!}{(n - c)!}, \tag{2.3b}$$

$$W(n, -1) = \gamma n. \tag{2.3c}$$

Substituting (2.3) into (2.2), we find

$$\frac{\partial P(n,t)}{\partial t} = \frac{\lambda}{b!} \frac{(n - a)!}{(n - a - b)!} P(n - a, t)$$

$$+ \frac{\mu}{c!} \frac{(n + d)!}{(n + d - c)!} P(n + d, t)$$

$$+ \gamma(n + 1)P(n + 1, t)$$

$$- \left[ \frac{\lambda}{b!} \frac{n!}{(n - b)!} + \frac{\mu}{c!} \frac{n!}{(n - c)!} + \gamma n \right] P(n,t), \tag{2.4}$$

where it is understood that $P(n < 0, t) = 0$. The probability generating function [32] is defined as

$$G(p,t) = \sum_{n=0}^{\infty} p^n P(n,t), \tag{2.5}$$

where $p$ is an auxiliary variable, which is conjugate to the number of particles [42]. Once $G(p,t)$ is known, the PDF is given by the Taylor coefficients

$$P(n,t) = \frac{1}{n!} \left[ \frac{\partial^n G(p,t)}{\partial p^n} \right]_{p=0}. \tag{2.6}$$

Normalization of $P(n,t)$ implies that $G(p = 1,t) = 1$. Multiplying (2.4) by $p^n$, summing over $n$, and renaming the index of summation, we find

$$\frac{\partial G(p,t)}{\partial t} = \frac{\lambda}{b!} \sum_{n=0}^{\infty} (p^{n+a} - p^n) \frac{n!}{(n - b)!} P(n,t)$$

$$+ \frac{\mu}{c!} \sum_{n=0}^{\infty} (p^{n-d} - p^n) \frac{n!}{(n - c)!} P(n,t)$$

$$+ \gamma \sum_{n=0}^{\infty} (p^{n-1} - p^n) n P(n,t). \tag{2.7}$$

Taking into account the property

$$p^k \frac{\partial^k G(p,t)}{\partial p^k} = \sum_{n=0}^{\infty} n(n - 1) \cdots (n - k + 1) p^n P(n,t)$$

$$= \sum_{n=0}^{\infty} \frac{n!}{(n - k)!} p^n P(n,t) \tag{2.8}$$

in (2.7), we finally obtain the evolution equation for $G(p,t)$,

$$\frac{\partial G(p,t)}{\partial t} = \frac{\lambda}{b!} p^b (p^a - 1) \frac{\partial^b G}{\partial p^b}$$

$$+ \frac{\mu}{c!} p^{c-d} (1 - p^d) \frac{\partial^c G}{\partial p^c} + \gamma(1 - p) \frac{\partial G}{\partial p}. \tag{2.9}$$

Equation (2.9) is exact and equivalent to the master equation (2.4). If only one individual reactant is present in all the reactions, i.e., $b = c = 1$, then (2.9) is first order in $p$ and can be solved exactly using the method of characteristics.

Macroscopic equations, i.e., equations for the expected or average values, can be obtained easily from (2.4). Multiplying

(2.4) by $n^k$, summing up over $n$, and renaming the index of summation, we find

$$\frac{\partial}{\partial t} \sum_{n=0}^{\infty} n^k P(n,t) = \frac{\lambda}{b!} \sum_{n=0}^{\infty} [(n+a)^k - n^k] \frac{n!}{(n-b)!} P(n,t)$$

$$+ \frac{\mu}{c!} \sum_{n=0}^{\infty} [(n-d)^k - n^k] \frac{n!}{(n-c)!} P(n,t)$$

$$+ \gamma \sum_{n=0}^{\infty} [(n-1)^k - n^k] n P(n,t). \quad (2.10)$$

The $k$th moment is defined as $\langle n^k \rangle = \sum_{n=0}^{\infty} n^k P(n,t)$ and evolves according to the ordinary differential equation

$$\frac{d\langle n^k \rangle}{dt} = \frac{\lambda}{b!} \left\langle [(n+a)^k - n^k] \prod_{m=0}^{b-1} (n-m) \right\rangle$$

$$+ \frac{\mu}{c!} \left\langle [(n-d)^k - n^k] \prod_{m=0}^{c-1} (n-m) \right\rangle$$

$$+ \gamma \langle [(n-1)^k - n^k] n \rangle. \quad (2.11)$$

Equation (2.11) is not closed and one must deal with a hierarchy of coupled differential equations for $k = 1,2,3,\ldots$. In order to truncate this set and to obtain closed equations, we make use of the mean-field approximation $\langle n^k \rangle \simeq \langle n \rangle^k$, which holds if the typical population size is large [31,32]. For $k = 1$, the mean-field equation reads

$$\frac{d\rho}{dt} = \frac{\lambda a}{b!} \rho^b - \frac{\mu d}{c!} \rho^c - \gamma \rho, \quad (2.12)$$

where $\rho = \langle n \rangle$ is a macroscopic quantity, the average or expected number of individuals in the population.

## III. BIRTH AND DEATH-BY-COMPETITION PROCESSES

We consider the case of two reactions, i.e., $\gamma = 0$:

$$bX \xrightarrow{\lambda} (b+a)X, \quad (3.1a)$$

$$cX \xrightarrow{\mu} (c-d)X. \quad (3.1b)$$

In the first reaction (birth), $b$ individuals have to interact with each other to produce $a$ new individuals at a constant rate $\lambda$. In the second reaction (death by competition), $c$ individuals interact with each other to remove $d$ individuals at a constant rate $\mu$. The fact that $b$, in general, can be larger than 1 includes scenarios where a single individual cannot generate by itself new individuals, which represents a type of Allee effect [43].

Equation (2.12) reduces to the logistic equation if $b = 1$ and $c = 2$. From a kinetic point of view this means that an individual does not need to interact to give rise to new individuals; the birth reaction takes the form $X \xrightarrow{\lambda} (a+1)X$. The fact $c = 2$ implies that a linear death rate, corresponding to $X \rightarrow \emptyset$, cannot occur for the scheme (3.1) in this case. The possible death reactions, compatible with a mean-field logistic equation, are $2X \xrightarrow{\mu} X$ (competition) or $2X \xrightarrow{\mu} \emptyset$ (annihilation). Consequently, the birth-and-death processes that lead to logistic macroscopic behavior are

$$X \xrightarrow{\lambda} (a+1)X, \quad (3.2a)$$

$$2X \xrightarrow{\mu} X \quad (3.2b)$$

and

$$X \xrightarrow{\lambda} (a+1)X, \quad (3.3a)$$

$$2X \xrightarrow{\mu} \emptyset. \quad (3.3b)$$

The logistic equation for these two reaction schemes reads

$$\frac{d\rho}{dt} = r\rho \left(1 - \frac{\rho}{N}\right), \quad (3.4)$$

where

$$r \equiv a\lambda, \quad N \equiv 2a\lambda/\mu d \quad (3.5)$$

are the intrinsic growth rate and the carrying capacity, respectively. These definitions are valuable because they allow us to relate the macroscopic parameters $r$ and $N$, which can be measured for different kinds of populations, to the microscopic parameters that characterize the stochastic processes involved in the interaction between the individuals of the population. From a macroscopic point of view, the logistic equation for population growth is specified by two parameters. On the other hand, the schemes (3.2) and (3.3) contain up to four microscopic parameters, namely $a$, $d$, $\mu$ and $\lambda$. As a result, we have two additional free microscopic parameters that can take arbitrary positive values compatible with the same mean-field logistic equation. The rate equation (3.4) has an unstable steady state at $\rho_s = 0$ and a stable steady state at $\rho_s = N$ for $d = 1$ or $d = 2$. Below we deal separately with schemes (3.2) and (3.3) and apply the momentum-space ($p$-space) spectral theory to find the stationary PDF in the case of population survival or the MET in the case of population extinction. An important advantage of the $p$-space representation stems from the fact that the evolution equation for the generating function $G(p,t)$ is exactly equivalent to the original master equation. Therefore, the $p$-space approach is especially valuable for an exact analysis.

### A. The case $X \xrightarrow{\lambda} (a+1)X$ and $2X \xrightarrow{\mu} X$

In this case we expect the population to evolve to a nontrivial steady state and not to become extinct. The equation for the probability generating function (2.9) becomes

$$\frac{\partial G(p,t)}{\partial t} = \lambda p(p^a - 1) \frac{\partial G}{\partial p} + \frac{\mu}{2}(p - p^2) \frac{\partial^2 G}{\partial p^2}. \quad (3.6)$$

If initially at $t = 0$ the system consists of $n_0$ individuals, then $P(n,0) = \delta_{n,n_0}$, where $\delta$ is the Kronecker delta, and from (2.5) we find $G(p,t = 0) = p^{n_0}$. The boundary conditions (BCs) are self-generated. Indeed, the equality $G(p = 1,t) = 1$ holds at all times, due to the conservation of probability. Equation (3.6) has a singular point at $p = 0$. Since $G(p,t)$ must be an analytic function at $p = 0$ for all times, we require that $G(p = 0,t) = 0$. This condition stems from the fact that $G(p = 0,t) = P_0(t)$ and since the population cannot go extinct, the probability of extinction vanishes at all times. We
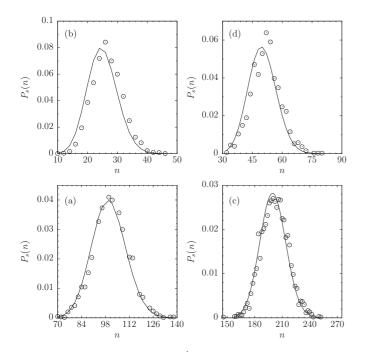
FIG. 1. Stationary PDF for $X \xrightarrow{\lambda} 2X$ and $2X \xrightarrow{\mu} X$ with (a) $N = 100$, (b) $N = 25$, (c) $N = 200$, and (d) $N = 50$. Simulation results (symbols) are based on 3000 realizations of the stochastic process up to time $10^6$.



FIG. 2. Stationary PDF for $X \xrightarrow{\lambda} 3X$ and $2X \xrightarrow{\mu} X$ with (a) $N = 200$, (b) $N = 50$, (c) $N = 400$, and (d) $N = 100$. Simulation (symbols) results are based on 3000 realizations of the stochastic process up to time $10^6$.

are interested in the steady state. Then (3.6) turns into

$$\frac{\mu}{2}(1-p)G_s'' + \lambda(p^a - 1)G_s' = 0, \qquad (3.7)$$

which must be solved with the BCs $G_s(1) = 1$ and $G_s(0) = 0$. The exact analytical solution reads

$$G_s(p) = \frac{\int_0^p \exp[N\phi(s)/a]ds}{\int_0^1 \exp[N\phi(s)/a]ds}, \qquad (3.8)$$

where

$$\phi(s) = -\ln(1-s) - \int \frac{s^a}{1-s}ds = \sum_{n=1}^{a} \frac{s^n}{n} \qquad (3.9)$$

and $N = 2a\lambda/\mu$. In the special case where $a = 1$, the exact solution for the generating function can be easily obtained from (3.8) and (3.9),

$$G_s(p) = \frac{\exp(Np) - 1}{\exp(N) - 1}. \qquad (3.10)$$

Expanding $\exp(Np)$ around $p = 0$, we find that for large $N$ the stationary PDF follows the Poisson distribution

$$P_s(n) = \frac{N^n \exp(-N)}{n!}, \qquad (3.11)$$

where we have approximated $\exp(N) - 1 \simeq \exp(N)$ in the denominator. We have performed numerical simulations and compared them with (3.11). Figure 1 shows that the agreement becomes better as the typical number of individuals $N$ is increased.
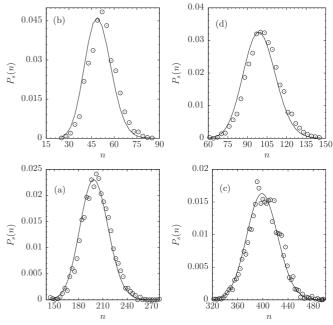
If $a = 2$, the generating function is given by

$$G_s(p) = \frac{\mathrm{erfi}(\sqrt{N}/2) - \mathrm{erfi}(\sqrt{N}(1+p)/2)}{\mathrm{erfi}(\sqrt{N}/2) - \mathrm{erfi}(\sqrt{N})}, \qquad (3.12)$$

where $\mathrm{erfi}(x) = \frac{2}{\sqrt{\pi}}\int_0^x \exp(t^2)dt$. The PDF can be obtained by substituting (3.12) into (2.6). A comparison between the analytical PDF and numerical simulations is shown in Fig. 2 and excellent agreement is observed.

Finally, we can also obtain the mean number of individuals in the stationary state and its dependence on $N = 2a\lambda/\mu$ by using the definition of $G$ from (2.5). Differentiating (3.8) with respect to $p$ and using (3.9), we find

$$\langle n \rangle = G'(1) = \frac{\exp[(N/a)\phi(1)]}{\int_0^1 \exp[(N/a)\phi(s)]ds}. \qquad (3.13)$$

Furthermore, the variance of $n$ satisfies $\langle n^2 \rangle - \langle n \rangle^2 = G''(1) + G'(1) - G'(1)^2$ and we find

$$\langle n^2 \rangle - \langle n \rangle^2 = \langle n \rangle(1 + N) - \langle n \rangle^2. \qquad (3.14)$$

This allows us to determine the coefficient of variation $c_v$, defined as the ratio of the standard deviation to the mean, which measures the variability in relation to the mean of the population

$$c_v \equiv \frac{\sqrt{\langle n^2 \rangle - \langle n \rangle^2}}{\langle n \rangle} = \sqrt{\frac{(1+N)}{\langle n \rangle} - 1}. \qquad (3.15)$$

In Fig. 3 we plot the coefficient of variation $c_v$ obtained from numerical simulations (circles) and compare it with the theoretical result given by (3.15).

It is straightforward to obtain asymptotic expressions for the mean, the variance, and the coefficient of variation if $N$ is
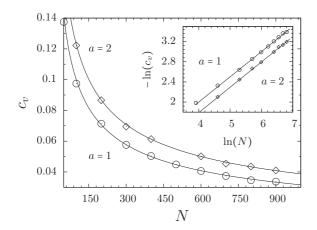
FIG. 3. Coefficient of variation $c_v$ versus $N$ for $a = 1$ and $a = 2$. The log-log plot in the inset shows that $c_v$ decays like $N^{-1/2}$. Simulation results are based on 3000 realizations of the stochastic process up to time $10^6$. We set $\mu = 2$ and $d = 1$ and vary $\lambda$.

large. In that case, the integral in the denominator of (2.9) can be evaluated by integration by parts for Laplace integrals and we find

$$\int_0^1 \exp\left[\frac{N}{a}\phi(s)\right]ds \simeq \frac{1}{N}\left(\exp\left[\frac{N}{a}\phi(1)\right] - a\right). \quad (3.16)$$

As a result, the mean value reads

$$\langle n \rangle \simeq N\left(1 + a\exp\left[-\frac{N}{a}\phi(1)\right] + \cdots\right) \quad (3.17)$$

and the coefficient of variation is given by

$$c_v = \frac{1}{\sqrt{N}}\left(1 - \frac{a}{2}N\exp\left[-\frac{N}{a}\phi(1)\right] + \cdots\right). \quad (3.18)$$

### B. The case $X \xrightarrow{\lambda} (a+1)X$ and $2X \xrightarrow{\mu} \emptyset$

In this case, the initial number of individuals and the parameter $a$ play a crucial role in determining the ultimate fate of the population. Since the death process involves two individuals, population extinction is guaranteed, regardless of the initial number of individuals, if the number of newborn individuals $a$ is odd, i.e., $a + 1$ is even. In contrast, if $a$ is even, i.e., $a + 1$ is odd, the population becomes extinct only if $n_0$ is even.

#### 1. The case when a is even and $n_0$ is odd

We begin by considering the case that $a$ is even. Then the birth process preserves the even-odd parity of the number of particles. As a result, the population becomes eventually extinct if the initial number of individuals $n_0$ is even. If $n_0$ is odd, the case considered in this section, the population evolves to a nontrivial stationary state. The equation for the probability generating function (2.9) is given by

$$\frac{\partial G(p,t)}{\partial t} = \lambda p(p^a - 1)\frac{\partial G}{\partial p} + \frac{\mu}{2}(1 - p^2)\frac{\partial^2 G}{\partial p^2}. \quad (3.19)$$

The boundary condition $G(p = 1,t) = 1$ still applies, but the singular point of (3.19) occurs at $p = -1$ and not at $p = 0$

as in (3.6). Since $G(p,t)$ must be analytic at $p = -1$ for all times, we require that $G(p = -1,t) = (-1)^{n_0}$. This boundary condition stems from the fact that $G(p = -1,t)$ is the sum of all even probabilities minus the sum of all odd probabilities [36]. The steady state has to be solved by integrating the equation

$$\frac{\mu}{2}(1 - p^2)G_s'' + \lambda p(p^a - 1)G_s' = 0, \quad (3.20)$$

with the boundary conditions $G_s(1) = 1$ and $G_s(-1) = (-1)^{n_0}$. The exact solution reads

$$G_s(p) = C_1\int^p \exp[N\varphi(s)/a]ds + C_2, \quad (3.21)$$

where

$$\varphi(s) = -\ln(1 - s^2) - 2\int\frac{s^{a+1}}{1-s^2}ds \quad (3.22)$$

and $N = a\lambda/\mu$. For $n_0$ odd, we obtain from the boundary conditions

$$C_1 = \frac{2}{\int_{-1}^1 \exp[N\varphi(s)/a]ds} \quad (3.23)$$

and

$$C_2 = 1 - \frac{2}{\int_{-1}^1 \exp[N\varphi(s)/a]ds}. \quad (3.24)$$

As expected, the system reaches a nontrivial stationary state with

$$G_s(p) = 1 + 2\frac{\int_1^p \exp[N\varphi(s)/a]ds}{\int_{-1}^1 \exp[N\varphi(s)/a]ds}. \quad (3.25)$$

To be specific, we focus on the case $a = 2$, that is, $X \xrightarrow{\lambda} 3X$ and $2X \xrightarrow{\mu} \emptyset$. From (3.22) we obtain $\varphi(s) = s^2$ and from (3.25)

$$G_s(p) = \frac{\text{erfi}(\sqrt{2N}p/2)}{\text{erfi}(\sqrt{2N}/2)}. \quad (3.26)$$

The PDF is obtained by substituting (3.26) into (2.6). In Fig. 4 we plot the PDF $P_s(n)$ for different values of $N$.

In Fig. 5 we plot the coefficient of variation $c_v$ for the cases of $a = 2$ and $a = 4$. The mean number of individuals in the steady state $\langle n \rangle = G'(1)$ can be determined from (3.26),

$$\langle n \rangle = \frac{\sqrt{2N}\exp(N/2)}{\sqrt{\pi}\,\text{erfi}(\sqrt{2N}/2)}, \quad (3.27)$$

and the coefficient of variation is given by (3.15) with $\langle n \rangle$ given by (3.27). The solid curve corresponds to the analytical results and the symbols correspond to numerical simulations. The inset again shows that $c_v$ scales like $N^{-1/2}$.

#### 2. The case when a and $n_0$ are even

If $n_0$ is even, the boundary conditions lead to

$$C_1\int^1 \exp[N\varphi(s)/a]ds + C_2 = 1 \quad (3.28)$$
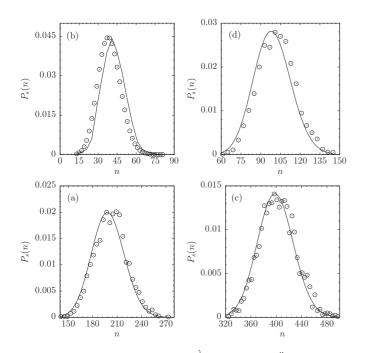
and

$$C_1\int^{-1} \exp[N\varphi(s)/a]ds + C_2 = 1, \quad (3.29)$$

FIG. 4. Stationary PDF for $X \xrightarrow{\lambda} 3X$ and $2X \xrightarrow{\mu} \emptyset$ with (a) $N = 200$, (b) $N = 40$, (c) $N = 400$, and (d) $N = 100$. Simulation (symbols) results are based on 3000 realizations of the stochastic process up to time $10^6$.

so that $C_1 = 0$ and $C_2 = 1$. Therefore, $G_s(p) = 1$, which describes an empty population state, i.e., extinction, as $t \to \infty$. To calculate the MET, we employ the momentum-space spectral method developed recently [36,37,42,44]. After a short relaxation time $t_r$, which corresponds to the deterministic relaxation time of the system to the stable stationary state, the population typically settles into a long-lived metastable state, which is encoded by the lowest excited eigenmode $\psi(p)$ of the probability generating function $G(p,t)$ [44]. Indeed, for $t \gg t_r$, we can write

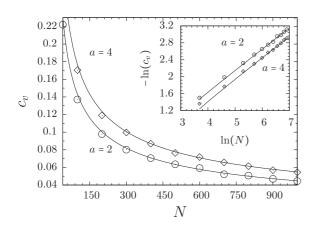$$G(p,t) = G_s(p) - \psi(p)\exp(-\mu E_1 t). \quad (3.30)$$



FIG. 5. Coefficient of variation versus $N$ for $a = 2$ and $a = 4$. The inset demonstrates that $c_v$ decays like $N^{-1/2}$. Simulation results are based on 3000 realizations of the stochastic process up to time $10^6$. We set $\mu = d = 2$ and vary $\lambda$.

Here $E_1$ is the lowest nonzero eigenvalue, $\tau = (\mu E_1)^{-1}$ is the mean time to extinction, and $G_s(p) = 1$. Substituting (3.30) into (3.6), we obtain

$$(1 - p^2)\psi''(p) + 2\Omega p(p^a - 1)\psi'(p) = -2E_1\psi(p), \quad (3.31)$$

where $\Omega \equiv \lambda/\mu$. Since $a$ is even, the function $\psi(p)$ is also an even function. It is therefore sufficient to consider the interval $0 \leqslant p < 1$. Since $\langle n \rangle \sim \Omega$, we assume that $\Omega \gg 1$ to find the eigenvalue $E_1$, which we expect to be exponentially small in $\Omega$. We will proceed by matching the asymptotic expansion for the function $\psi(p)$ in the bulk region $0 \leqslant p < 1$, namely, $\psi_b$, with $\psi_l$, the solution in the boundary layer $1 - p \ll 1$. We will show that the function $\psi(p)$ is almost constant everywhere within the interval $p \in [0,1)$, except in a narrow layer close to $p = 1$. In the bulk we can treat $E_1$ as a perturbative parameter. To zeroth order we set $E_1 = 0$ and the even solution of (3.31) is 1. To account for corrections, we write $\psi(p) = 1 + \delta\psi$, where $\delta\psi \ll 1$ satisfies the differential equation

$$\delta\psi'' + 2\Omega p\frac{p^a - 1}{1 - p^2}\delta\psi' = -\frac{2E_1}{1 - p^2}, \quad (3.32)$$

whose solution, using Eq. (3.22), takes the form

$$\delta\psi'(p) = C_0 \exp[\Omega\varphi(p)] - 2E_1 \exp[\Omega\varphi(p)]$$
$$\times \int^p \frac{\exp[-\Omega\varphi(s)]}{1 - s^2}ds. \quad (3.33)$$

To solve for $\psi(p)$, we need to specify two boundary conditions. Setting $p = 0$ in (3.31), we obtain $\psi''(0) = -2E_1\psi(0)$ or equivalently $\delta\psi''(0) = -2E_1 - 2E_1\delta\psi(0)$. On the other hand, from (3.32) and setting $p = 0$, we find the first boundary condition $\delta\psi''(0) = -2E_1$. This condition together with $\delta\psi''(0) = -2E_1 - 2E_1\delta\psi(0)$ leads to the second boundary condition $\delta\psi(0) = 0$. The first boundary condition implies that (3.33) reduces to

$$\delta\psi'(p) = -2E_1 \exp[\Omega\varphi(p)]\int_0^p \frac{\exp[-\Omega\varphi(s)]}{1 - s^2}ds, \quad (3.34)$$

which can be integrated together with the second boundary condition to yield

$$\delta\psi(p) = -2E_1\int_0^p \exp[\Omega\varphi(s)]ds\int_0^s \frac{\exp[-\Omega\varphi(u)]}{1 - u^2}du. \quad (3.35)$$

Since this solution holds in the bulk region $1 - p \gg \Omega^{-1}$, with $\Omega \gg 1$, we can approximate the inner integral in (3.35) as

$$\int_0^s \frac{\exp[-\Omega\varphi(u)]}{1 - u^2}du \simeq \int_0^s \exp[-\Omega\varphi(u)]du$$
$$\simeq \int_0^\infty \exp[-\Omega\varphi(u)]du. \quad (3.36)$$

Therefore,

$$\psi_b(p) \simeq 1 - 2E_1\int_0^p \exp[\Omega\varphi(s)]ds\int_0^\infty \exp[-\Omega\varphi(u)]du.$$
$$(3.37)$$

In the boundary layer $1 - p \ll 1$ we disregard the exponentially small term $E_1\psi$ in (3.31) and integrate the resulting

equation $(1 - p^2)\psi''(p) + 2\Omega p(p^a - 1)\psi'(p) = 0$ to obtain

$$\psi_l(p) = C \int_1^p \exp[\Omega\varphi(s)]ds, \quad (3.38)$$

where we have made use of the boundary condition at the boundary layer, i.e., $\psi_l(1) = 0$. Equation (3.38) can be rewritten as

$$\psi_l(p) = C\left(\int_0^p \exp[\Omega\varphi(s)]ds - \int_0^1 \exp[\Omega\varphi(s)]ds\right)$$

$$= C_1\left(1 - \frac{\int_0^p \exp[\Omega\varphi(s)]ds}{\int_0^1 \exp[\Omega\varphi(s)]ds}\right). \quad (3.39)$$

Matching the solutions (3.37) and (3.39), we find $C_1 = 1$ and the MET

$$\tau = \frac{2}{\mu} \int_0^1 \exp[\Omega\varphi(s)]ds \int_0^\infty \exp[-\Omega\varphi(u)]du. \quad (3.40)$$

Since $\Omega \gg 1$, we can further approximate (3.40). The function $\varphi(s)$, given by (3.22), can be expressed as

$$\varphi(s) = \sum_{j=1}^{a/2} \frac{s^{2j}}{j} \quad (3.41)$$

for even $a$ and

$$\varphi(s) = -2\ln(1 + s) + 2 \sum_{j=0}^{(a-1)/2} \frac{s^{2j+1}}{2j+1} \quad (3.42)$$

for odd $a$. Since in this section we consider the case of even $a$, $\varphi(s)$ is a polynomial of order $a$ with positive coefficients. Therefore, the main contribution of the first integral in (3.40) comes from the region around $s = 1$. Employing the Taylor expansion, we find

$$\int_0^1 \exp[\Omega\varphi(s)]ds \simeq \int_0^1 \exp\{\Omega[\varphi(1) + \varphi'(1)(s-1)]\}ds$$

$$\simeq \frac{\exp[\Omega\varphi(1)]}{\Omega\varphi'(1)}. \quad (3.43)$$

For the second integral in (3.40), the main contribution comes from the region around $u = 0$. To leading order, $\varphi(u) \simeq u^2$ and

$$\int_0^\infty \exp[-\Omega\varphi(u)]du \simeq \int_0^\infty \exp[-\Omega u^2]du = \frac{\sqrt{\pi}}{2\sqrt{\Omega}}. \quad (3.44)$$

Substituting these results into (3.40), we obtain a general result for the MET for $\Omega \gg 1$ and any even $a$,

$$\tau = \frac{\sqrt{\pi}\exp\left(\Omega \sum_{j=1}^{a/2}(1/j)\right)}{\mu a \Omega^{3/2}}. \quad (3.45)$$

As an example, for $a = 2$ we find

$$\tau = \frac{\sqrt{\pi}\exp(\Omega)}{2\mu\Omega^{3/2}}, \quad (3.46)$$

which coincides with the result in [36]. We have verified the result (3.45) by numerical simulations. In Fig. 6(b) we plot $\tau$ versus $N$ for $a = 2$ and $a = 4$ and in Fig. 6(a) we plot $\tau$ versus $a$ for different values of $\Omega$. In all these comparisons we obtain excellent agreement between theory and simulations.
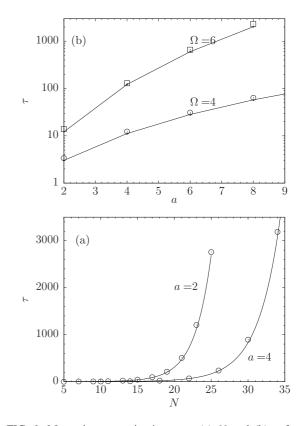


FIG. 6. Mean time to extinction $\tau$ vs (a) $N$ and (b) $a$ for the reactions $X \xrightarrow{\lambda} (a+1)X$ and $2X \xrightarrow{\mu} \emptyset$. Solid curves are obtained from (3.45), while symbols correspond to numerical simulations. We set $\mu = 2$ and vary $\lambda$. Simulations have been performed up to time $10^8$.

### 3. The case when $a$ is odd

If $a$ is odd, (3.19) has no other singularity and we have only one boundary condition $G_s(1) = 1$. As a result, $G_s(p) = 1$ and the population becomes extinct, regardless of the value of $n_0$. To obtain the MET in this case, we start again with (3.19). Since $\psi(p)$ is no longer even, the bulk region now corresponds to $p \in [-1,1)$ and the boundary layer is located at $1 - p \ll 1$. In the bulk region we impose the boundary condition $\delta\psi(0) = 0$, as in the case of even $a$. However, setting $p = -1$ in (3.31), we find now the second boundary condition to be $\psi'(-1) = 0$, where we have neglected the term $E_1\psi(-1)$, which is exponentially small. The final solution for the function $\psi$ in the bulk region is very similar to the even $a$ case and we find

$$\psi_b(p) = 1 - 2E_1 \int_0^p \exp[\Omega\varphi(s)]ds \int_{-1}^s \frac{\exp[-\Omega\varphi(u)]}{1 - u^2}du. \quad (3.47)$$

In the boundary layer we obtain exactly the same result as (3.38). By matching both solutions in the common region we obtain

$$\tau = \frac{2}{\mu} \int_0^1 \exp[\Omega\varphi(s)]ds \int_{-1}^\infty \frac{\exp[-\Omega\varphi(u)]}{1 - u^2}du. \quad (3.48)$$
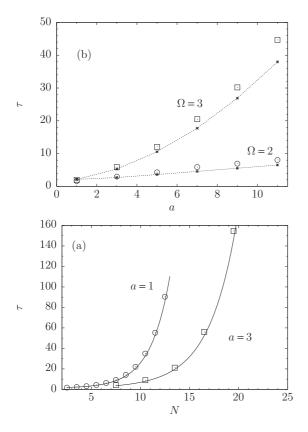
FIG. 7. Mean time to extinction $\tau$ vs (a) $N$ and (b) $a$ for the reactions $X \xrightarrow{\lambda} (a+1)X$ and $2X \xrightarrow{\mu} \emptyset$. Solid curves are obtained from (3.50), while symbols correspond to numerical simulations. We set $\mu = 2$ and vary $\lambda$. Simulations have been performed up to time $10^8$.

To proceed, we employ the approximations (3.36) and

$$\int_{-1}^{s} \frac{\exp[-\Omega \varphi(u)]}{1 - u^2} du \simeq \int_{-1}^{s} \exp[-\Omega \varphi(u)] du$$

$$\simeq \int_{-1}^{\infty} \exp[-\Omega \varphi(u)] du$$

$$\simeq \int_{-1}^{\infty} \exp[-\Omega u^2] du = \frac{\sqrt{\pi}}{\sqrt{\Omega}}. \quad (3.49)$$

As a result, similar to the even $a$ case, we obtain from (3.42) the general result for any odd $a$,

$$\tau = \frac{2\sqrt{\pi}}{\mu a \Omega^{3/2}} \exp\left(-2\Omega \ln 2 + 2\Omega \sum_{j=0}^{(a-1)/2} \frac{1}{2j+1}\right). \quad (3.50)$$

For $a = 1$, (3.50) yields

$$\tau = \frac{2\sqrt{\pi} \exp[2\Omega(1 - \ln 2)]}{\mu \Omega^{3/2}}, \quad (3.51)$$

which coincides with the result in [37].

In Fig. 7 we verify the result (3.50) for the MET. In Fig. 7(a) we plot $\tau$ versus $N$ for $a = 1$ and $a = 3$. The mean time to extinction increases as the number of individuals increases, as expected. In Fig. 7(b) we plot $\tau$ versus $a$ for relatively low values of $\Omega$ and the agreement between theory and numerical simulations is still fair.

## IV. BIRTH-COMPETITION-DEATH PROCESSES

We add the death reaction $X \xrightarrow{\gamma} \emptyset$ to the system of birth-competition processes (3.1). To obtain a logistic equation in the mean-field limit, we consider $b = 1$ and $c = 2$, leading to the reaction scheme

$$X \xrightarrow{\lambda} (a+1)X, \quad (4.1a)$$

$$2X \xrightarrow{\mu} (2-d)X, \quad (4.1b)$$

$$X \xrightarrow{\gamma} \emptyset. \quad (4.1c)$$

Here $a \geqslant 1$ and $d = 1$ for a birth-competition-death system and $d = 2$ for a birth-annihilation-death system. It is straightforward to show that this system always goes extinct. We are interested in calculating the MET for the general case. Although this can also be done via the generating function ($p$-space theory), we will use the real-space WKB approximation [26,45–48]. According to (2.3), the transition rates are given by

$$W(n, a) = \lambda n, \quad (4.2a)$$

$$W(n, -d) = \frac{\mu}{2} \frac{n!}{(n-2)!} = \frac{\mu}{2} n(n-1), \quad (4.2b)$$

$$W(n, -1) = \gamma n. \quad (4.2c)$$

Replacing $t$ by $t/\gamma$ and introducing the rescaled population number density $q = n/N$, where $N = \lambda/\mu \gg 1$, the transition rates can be rewritten as

$$W(n, r) \equiv W(Nq, r) = N w_r(q) + u_r(q) + O(N^{-1}), \quad (4.3)$$

where

$$w_a(q) = R_0 q, \quad (4.4a)$$

$$w_{-d}(q) = \frac{1}{2} R_0 q^2, \quad (4.4b)$$

$$w_{-1}(q) = q. \quad (4.4c)$$

Here $q$, $w_r(q)$, and $u_r(q)$ are $O(1)$ and

$$u_a(q) = u_{-1}(q) = 0, \quad (4.5a)$$

$$u_{-d}(q) = -\frac{1}{2} R_0 q. \quad (4.5b)$$

Further, $R_0 = \lambda/\gamma$ is the basic reproductive number. Since $n = q = 0$ is an absorbing state (extinction), we have $w_r(0) = u_r(0) = 0$ for any $r = \{a, -d, -1\}$. For $N \gg 1$, the WKB theory developed in [26,45–48] can be used for the rescaled master equation. Accordingly, we look for the probability $P(n, t) = P(Nq, t)$ in the form of the WKB ansatz

$$P(q, t) = \exp[-N S(q)], \quad (4.6)$$

where $S(q)$ is a deterministic state function known as the action. Intuitively, this approximation expresses the assumption that the probability of occurrence of extreme events, such as extinction, lies in the tail of the PDF, which falls away steeply from the steady state. Substituting (4.6) into the rescaled master equation (2.4), which contains terms of the form $w_r(q - r/N)$, and Taylor-expanding terms such as $S(q - r/N)$ around $q$, we obtain to leading order a Hamilton-Jacobi

equation $H(p,q) = 0$ [45], with the Hamiltonian

$$H(p,q) = \sum_r w_r(q)[\exp(rp) - 1] = R_0 q[\exp(ap) - 1]$$
$$+ \frac{R_0}{2}q^2[\exp(-dp) - 1] + q[\exp(-p) - 1]. \tag{4.7}$$

Here $q$ is the coordinate and $p = S'(q)$ is the conjugate momentum. The mean-field dynamics can be found by writing the Hamilton equation $\dot{q} = \partial_p H$ along the path $p = 0$. This yields the logistic equation as the mean-field description of the system (4.1),

$$\frac{dq}{dt} = \left(\frac{\partial H}{\partial p}\right)_{p=0} = \sum_r r w_r(q) = q\left(aR_0 - 1 - \frac{dR_0}{2}q\right). \tag{4.8}$$

where $q = \langle n \rangle / N$. Equation (4.8) has an nontrivial attracting steady state at

$$q_* = \frac{2}{d}(a - 1/R_0) \tag{4.9}$$

if

$$aR_0 > 1. \tag{4.10}$$

Note that a bifurcation occurs at $R_0 = 1/a$. This implies that the population can maintain a long-lived metastable state for $a > 1$, even if $R_0 < 1$. Returning to the (mean) number of individuals $n$, the logistic mean-field rate equation (4.8) reads

$$\frac{dn}{dt} = rn\left(1 - \frac{n}{K}\right), \tag{4.11}$$

where

$$r \equiv aR_0 - 1 = \frac{a\lambda - \gamma}{\mu} \tag{4.12}$$

and

$$K \equiv Nq_* = \frac{2(a\lambda - \gamma)}{d\mu} \tag{4.13}$$

are the intrinsic growth rate and the carrying capacity, respectively. The mean-field logistic equation is completely specified by the two parameters $r$ and $K$. On the other hand, the stochastic dynamics is characterized by up to five parameters, namely, $a$, $d$, $\lambda$, $\mu$, and $\gamma$. Relations (4.12) and (4.13) provide a constraint for two of them and the other three are free to take different values while keeping exactly the same mean-field logistic equation.

In order to find the MET, we need to find the optimal path to extinction, which is defined as the nontrivial heteroclinic orbit that solves the equation $H(q,p) = 0$ in the phase space $(q,p)$ and connects the state $(q_*, p = 0)$ to the extinction state $(q = 0, p = p_f)$. Here $p_f$ is the solution to the equation $q_a(p_f) = 0$, namely, the value of the momentum along the optimal path to

extinction at the point where $q$ vanishes. For the system (4.1) we find the optimal path to extinction (activation trajectory)

$$q_a(p) = 2\frac{R_0[\exp(ap) - 1] - 1 + \exp(-p)}{R_0[1 - \exp(-dp)]} \tag{4.14}$$

and $p_f$ is the solution of the transcendental equation

$$R_0[\exp(ap_f) - 1] - 1 + \exp(-p_f) = 0. \tag{4.15}$$

According to [26], the MET is given by

$$\tau = \frac{A_1\sqrt{2\pi}}{\gamma q_*}\sqrt{\frac{q_a'(p=0)}{N}}\exp(N\Delta S)\exp(\Delta\phi), \tag{4.16}$$

where, taking into account (4.14),

$$\frac{1}{q_*}\sqrt{\frac{q_a'(p=0)}{N}} = \frac{\sqrt{dR_0}}{2(aR_0 - 1)}\sqrt{\frac{R_0 a(a+d) + 1 - d}{N}}. \tag{4.17}$$

The quantities $\Delta S$ and $\Delta\phi$ can be calculated as follows: $\Delta S$ is the action increment along the extinction path, which gives us the logarithm of the mean time to extinction [26]. Since $p = dS/dq$,

$$\Delta S = S(0) - S(q_*) = \int_{q_*}^0 p_a(q)dq = \int_{p_f}^0 q_a(p)dp. \tag{4.18}$$

Making use of (4.14), we obtain from (4.18)

$$\Delta S = S(0) - S(q_*)$$
$$= 2\int_{e^{p_f}}^1 \frac{z^{a+d} - (1 + R_0^{-1})z^d + R_0^{-1}z^{d-1}}{z(z^d - 1)}dz. \tag{4.19}$$

For $d = 1$, this equation yields

$$\Delta S = S(0) - S(q_*) = \frac{2p_f}{R_0} + 2\sum_{j=1}^a \frac{1}{j} - 2\sum_{j=1}^a \frac{\exp(jp_f)}{j}. \tag{4.20}$$

For $d = 2$, (4.19) yields, for even $a$,

$$\Delta S = S(0) - S(q_*) = 2\left(1 + \frac{1}{R_0}\right)\ln\left(\frac{1 + \exp(p_f)}{2}\right)$$
$$+ 2\sum_{j=1}^{a/2} \frac{1 - \exp(2jp_f)}{2j} \tag{4.21}$$

and for odd $a$,

$$\Delta S = S(0) - S(q_*) = 2\left(1 + \frac{1}{R_0}\right)\ln\left(\frac{1 + \exp(p_f)}{2}\right)$$
$$+ 2\sum_{j=1}^{(a+1)/2} \frac{1 - \exp[(2j-1)p_f]}{2j - 1}. \tag{4.22}$$

In order to go beyond leading-order calculations, we determine $\Delta\phi = \phi(q = 0) - \phi(q = q_*)$, using its definition given in [26],

$$\Delta\phi = \int_0^{p_f} q_a'(p)\left[\frac{H_{pq}(q_a,p) + (1/2)[q_a'(p)]^{-1}H_{pp}(q_a,p) + (R_0/2)q_a(p)[\exp(-dp) - 1]}{H_p(q_a,p)} - \frac{1}{q_a(p)}\right]dp, \tag{4.23}$$

where $q'_a(p) = dq_a/dp$ and the subscripts on $H$ indicate partial derivatives. Making use of (4.7) and (4.14), we obtain from (4.23), for $d = 1$,

$$\Delta\phi = -\frac{p_f}{2} - \frac{1}{2}\ln\left(\frac{1+a}{2}\right) + \frac{1}{2}\ln\left[\frac{a\exp[(a+1)p_f] - (1+a)\exp(ap_f) + 1}{a[\exp(p_f) - 1]^2}\right] \quad (4.24)$$

and for $d = 2$,

$$\Delta\phi = -\frac{p_f}{2} + \frac{1}{2}\ln\left[4\frac{aR_0\exp[p_f(a+3)] - R_0(a+2)\exp[p_f(a+1)] - \exp(2p_f) + 2(R_0+1)\exp(p_f) - 1}{(a^2R_0 + 2aR_0 - 1)[\exp(2p_f) - 1]^2}\right]. \quad (4.25)$$

The formula for the coefficient $A_1$ is given by [see Eq. (39) of [26]]

$$A_1 = \frac{(-1)^a \prod_{j=1}^a l_j}{(l_1 - 1)\prod_{j=2}^a (l_1 - l_j)}, \quad (4.26)$$

where $l_i$ are the roots of the equation

$$w'_a(0)l^{a+1} - [1 + w'_a(0)]l + 1 = 0. \quad (4.27)$$

Here we have used Eq. (31) of [26]. It can be shown that one root of this equation is always $l = 1$. We denote this root by $l_0$. Using the fact that $w'_a(0) = R_0$ and dividing by $l - 1$, we need to solve the equation $lR_0(1 + l + \cdots + l^{a-1}) - 1 = 0$, i.e.,

$$l + \cdots + l^a = \frac{1}{R_0}. \quad (4.28)$$

For $a = 1$, (4.28) has a single root and therefore (4.26) simplifies to $A_1^{(a=1)} = 1/(R_0 - 1)$. For $a = 2$, (4.28) has two roots and we find

$$A_1^{(a=2)} = \frac{2}{3\sqrt{R_0^2 + 4R_0} - R_0 - 4}. \quad (4.29)$$

For $a = 3$, the polynomial of (4.28) is of third order and its solution yields

$$A_1^{(a=3)} = \frac{(c+2)(4-c)(c^2 - 2c + 4)(c^2 + 4c + 16)}{3(c^2 - 8c - 8)(c^4 - 8c^2 + 64)}, \quad (4.30)$$

where

$$c = \left[4\frac{3\sqrt{3}\sqrt{3R_0^2 + 14R_0 + 27} + 7R_0 + 27}{R_0}\right]^{1/3}. \quad (4.31)$$

Note that the value of $A_1^{(a)}$ does not depend on $d$. The origin of this behavior lies in the fact that reactions without a linear term in $n$, such as (4.1b), do not play a role in the recursive solution of the master equation for small values of $n$ [26].

Exact analytic expressions for the MET can be obtained for some specific cases. For example, if $a = d = 1$ (the birth-competition-death process), the reactions are given by

$$X \xrightarrow{\lambda} 2X, \quad (4.32a)$$

$$2X \xrightarrow{\mu} X, \quad (4.32b)$$

$$X \xrightarrow{\gamma} \emptyset. \quad (4.32c)$$

Equation (4.16) yields for the MET

$$\tau = \frac{1}{\gamma}\sqrt{\frac{\pi}{N}}\frac{R_0^{3/2}}{(R_0 - 1)^2}\exp\left[2N\left(1 - \frac{1 + \ln R_0}{R_0}\right)\right], \quad (4.33)$$

recovering the result given by Eq. (70) in [26].

For $a = 2$ and $d = 1$, the reactions are again of birth-competition-death type,

$$X \xrightarrow{\lambda} 3X, \quad (4.34a)$$

$$2X \xrightarrow{\mu} X, \quad (4.34b)$$

$$X \xrightarrow{\gamma} \emptyset. \quad (4.34c)$$

In this case, (4.16) yields for the MET

$$\tau = \frac{1}{\gamma}\sqrt{\frac{\pi}{N}}\frac{R_0[3\sqrt{R_0(R_0+4)} + R_0 + 4]\sqrt{R_0 + 4 + \sqrt{R_0(R_0+4)}}}{2(2R_0 - 1)^2(R_0 + 4)}$$

$$\times \exp(2N\Delta S), \quad (4.35)$$

where

$$\Delta S = \frac{1}{R_0}\ln\left(\frac{2}{R_0 + \sqrt{R_0(R_0+4)}}\right)$$

$$+ \frac{(3R_0 - 2)\sqrt{R_0(R_0+4)} + 3R_0^2 + 4R_0 - 2}{[R_0 + \sqrt{R_0(R_0+4)}]^2}. \quad (4.36)$$

The difference between results (4.33) and (4.35) is due the value of $a$. Figure 8 shows that increasing $a$ by one unit increases the MET by several orders of magnitude. One can show that $\tau(a = 2)/\tau(a = 1) \sim \exp(N)$ as $R_0$ tends to infinity.

Finally, we consider the case $a = 1$ and $d = 2$,

$$X \xrightarrow{\lambda} 2X, \quad (4.37a)$$

$$2X \xrightarrow{\mu} \emptyset, \quad (4.37b)$$

$$X \xrightarrow{\gamma} \emptyset. \quad (4.37c)$$

In this case the reactions are of birth, annihilation, and death type. From (4.16) we find

$$\tau = \frac{2}{\gamma}\sqrt{\frac{\pi}{N}}\frac{R_0^{3/2}}{(R_0 - 1)^2(R_0 + 1)^{1/2}}$$

$$\times \exp\left\{2N\left[\left(1 + \frac{1}{R_0}\right)\ln\left(\frac{1 + R_0}{2R_0}\right) + 1 - \frac{1}{R_0}\right]\right\}, \quad (4.38)$$

recovering the result already obtained in [26]. In Fig. 8 we plot the case $a = d = 1$ and the case $a = 1$ and $d = 2$. The fact that for $d = 2$ we have annihilation, rather than competition as for $d = 1$, reduces the MET as one would expect. If we take $R_0$ to
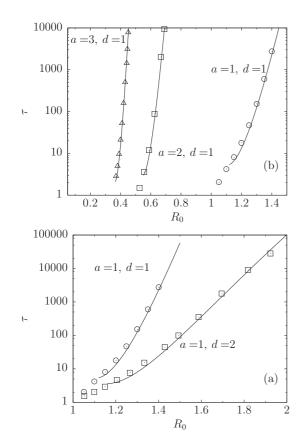
FIG. 8. Mean time to extinction for birth-and-death reactions. In both cases we set $\mu = 0.1$, $\lambda = 10$, $d = 1$, and $N = 100$ and modify $\gamma$ to vary $R_0$. We compare different values for the MET for (a) different $d$ and the same $a$ and (b) different $a$ and the same $b$. Simulations (symbols) have been performed up to time $10^9$ and mean values are obtained by averaging over $4 \times 10^4$ realizations. Solid curves correspond to exact analytic results given by (4.33), (4.35), and (4.38).

infinity and compare the cases of $d = 2$ and $d = 1$, both with $a = 1$, we find $\tau(d = 2)/\tau(d = 1) \sim \exp(-2N \ln 2)$. For both Figs. 8(a) and 8(b) we observe that the MET increases very fast with the basic reproductive number $R_0$. The comparison between simulations and analytic results is in general good, except when $R_0$ tends to the critical value given in (4.10). Indeed, the WKB theory breaks down if the barrier $\Delta S$ tends to zero. This happens if $p_f$ tends to 0. Considering (4.15), the limit $p_f \to 0$ implies $R_0 \to 1/a$.

## V. CONCLUSION

We have adopted an individual-based formulation to describe the random dynamics of finite-sized populations. Specifically, we have analyzed in detail various possible microscopic scenarios that all give rise to the same macroscopic population-level model, namely, the Verhulst or logistic population growth equation. We have shown that for birth and competition interactions between individuals $X \xrightarrow{\lambda} (a + 1)X$ and $2X \xrightarrow{\mu} X$, the population does not become extinct, regardless of the value of the parameters.

If competition leads to annihilation of the competitors $X \xrightarrow{\lambda} (a + 1)X$ and $2X \xrightarrow{\mu} \emptyset$, the ultimate fate of the population

depends on whether the kinetics is parity conserving or not. The parity of the total number of particles is preserved in the even-offspring case. This implies that the population persists if $a$ is even and $n_0$ is odd, because the absorbing state is inaccessible. On the other hand, if $a$ and $n_0$ are both even or if $a$ is odd, the absorbing state is accessible and the population becomes extinct. It is worth noting that these kinetic rules can be implemented as dynamical lattice models or interacting particle systems, for example, as a contact process or a branching-annihilating random walk (BARW) [49–55], and that parity conservation, or the lack thereof, also plays a crucial role in the dynamics of these spatially extended systems. They can display a nonequilibrium transition from a nontrivial fluctuating steady state to an absorbing state with no fluctuations [53]. This transition belongs to different universality classes for parity-conserving and nonparity-conserving models [56]. The most prominent member of the first class is the BARW with an even number of offsprings. The dynamics of BARWs with even and odd numbers of offsprings have been analyzed in detail in [57].

For those cases where the population persists, we have obtained analytic expressions for the generating function and the PDF in the stationary state. In particular, we have determined the mean of the PDF and its coefficient of variation. For those cases where the population becomes extinct, we have calculated the MET and have explored its dependence on the microscopic parameters. All our analytical results have been compared with numerical simulations, showing good agreement.

Our results provide further evidence for the advantages of individual-based models. They demonstrate that the microscopic details of random events at the level of the individuals lead to differences in the behavior of the system at the population level. In the case that the population persists, the characteristics of the stationary PDF depend on the features of the microscopic model. To illustrate this fact, we have focused on the coefficient of variation. Our results show (see Figs. 3 and 5) that an increase in $a$, the number of offsprings, and $d$, the number of individuals removed due to competition, leads to an increase in the variability of the population for the same value of the macroscopic parameter, the carrying capacity $N$. Measuring the coefficient of variation of a population for a given value of $N$ provides therefore a means of drawing inferences about the microscopic details of the birth and competition processes.

Similarly, in the case that the population becomes extinct, the MET depends sensitively on the microscopic details of the model, as illustrated by Figs. 6–8. For example, for the model $X \xrightarrow{\lambda} (a + 1)X$ and $2X \xrightarrow{\mu} \emptyset$, we find that the MET becomes significantly smaller for the same carrying capacity $N$ as $a$ increases, see Figs. 6 and 7. Extinction is always the ultimate fate for the birth-competition-death model $X \xrightarrow{\lambda} (a + 1)X$, $2X \xrightarrow{\mu} (2 - d)X$, and $X \xrightarrow{\gamma} \emptyset$. Figure 8 demonstrates strikingly the sensitive dependence of the MET on the microscopic details of the system. Measuring the MET for laboratory populations with a given basic reproductive number provides therefore a means of drawing inferences about the microscopic details of the birth, death, and competition processes. Our results also imply that assessing the extinction risks and

survival times of natural populations requires an understanding of the microscopic details of the processes that occur in the system and should not be based solely on phenomenological models.

There are many other possibilities that lead to the logistic equation, for example, if we consider two different birth reactions simultaneously, such as $X \xrightarrow{\lambda} 2X$ and $X \xrightarrow{\lambda} 3X$. Another possibility consists in considering schemes with four or even more reactions. All these situations can be analyzed in the same manner and with the same techniques as used here.

A further intriguing possibility that deserves study is reactions schemes where the number of offsprings $a$ and the number of individuals eliminated by exclusive competition $d$ fluctuate randomly between several values.

[1] V. Méndez, D. Campos, and F. Bartumeus, *Stochastic Foundations in Movement Ecology: Anomalous Diffusion, Invasion Fronts and Random Searches* (Springer, Heidelberg, 2014).

[2] L. J. S. Allen, *An Introduction to Stochastic Processes with Applications to Biology*, 2nd ed. (Chapman & Hall/CRC, Boca Raton, 2010).

[3] E. Renshaw, *Modelling Biological Populations in Space and Time* (Cambridge University Press, New York, 1993).

[4] P. F. Verhulst, Nouv. Mémoires de l'Académie Royale des Sciences et Belles Lettres de Bruxelles **18**, 1 (1845).

[5] P.-F. Verhulst, Mém. Acad. R. Sci. Lett. Beaux-Arts Belgique **20**, 1 (1847).

[6] R. Pearl and L. J. Reed, Proc. Natl. Acad. Sci. U.S.A. **6**, 275 (1920).

[7] V. Méndez, S. Fedotov, and W. Horsthemke, *Reaction-Transport Systems: Mesoscopic Foundations, Fronts, and Spatial Instabilities* (Springer, Heidelberg, 2010).

[8] W. Feller, Acta Biotheor. **5**, 11 (1939).

[9] D. G. Kendall, J. R. Stat. Soc. B **11**, 230 (1949).

[10] N. S. Goel and N. Richter-Dyn, *Stochastic Models in Biology* (Academic Press, New York, 1974).

[11] I. Nåsell, J. Theor. Biol. **211**, 11 (2001).

[12] O. N. Bjørnstad and B. T. Grenfell, Science **293**, 638 (2001).

[13] O. Ovaskainen and B. Meerson, Trends Ecol. Evol. **25**, 643 (2010).

[14] R. M. Nisbet, W. S. C. Gurney, and M. A. Pettipher, J. Theor. Biol. **68**, 143 (1977).

[15] G. Nicolis and I. Prigogine, *Self-Organization in Nonequilibrium Systems* (Wiley, New York, 1977).

[16] A. J. McKane and T. J. Newman, Phys. Rev. Lett. **94**, 218102 (2005).

[17] R. J. Kryscio and C. Lefévre, J. Appl. Probab. **26**, 685 (1989).

[18] I. Nåsell, J. R. Stat. Soc. B **61**, 309 (1999).

[19] M. J. Keeling and J. V. Ross, J. R. Soc. Interface **5**, 171 (2008).

[20] I. B. Schwartz, L. Billings, M. Dykman, and A. Landsman, J. Stat. Mech. (2009) P01005.

[21] T. Britton and P. Neal, J. Math. Biol. **61**, 763 (2010).

[22] T. Britton, Math. Biosci. **225**, 24 (2010).

[23] I. B. Schwartz, E. Forgoston, S. Bianco, and L. B. Shaw, J. R. Soc. Interface **8**, 1699 (2011).

[24] P. C. Bressloff, *Stochastic Processes in Cell Biology* (Springer, Cham, 2014).

[25] B. Dennis, P. L. Munholland, and J. M. Scott, Ecol. Monogr. **61**, 115 (1991).

[26] M. Assaf and B. Meerson, Phys. Rev. E **81**, 021116 (2010).

[27] B. A. Melbourne and A. Hastings, Nature (London) **454**, 100 (2008).

[28] C. Escudero, J. Buceta, F. J. de la Rubia, and K. Lindenberg, Phys. Rev. E **70**, 061907 (2004).

[29] A. J. Black and A. J. McKane, J. R. Soc. Interface **7**, 1219 (2010).

[30] M. Assaf and B. Meerson, Phys. Rev. Lett. **100**, 058105 (2008).

[31] N. G. Van Kampen, *Stochastic Processes in Physics and Chemistry* (Elsevier, Amsterdam, 1992).

[32] C. W. Gardiner, *Handbook of Stochastic Methods for Physics, Chemistry and the Natural Sciences* (Springer, Berlin, 1990).

[33] A. J. Black and A. J. McKane, Trends Ecol. Evol. **27**, 337 (2012).

[34] Y. R. Zelnik, S. Solomon, and G. Yaari, Sci. Rep. **5**, 7877 (2015).

[35] R. Toral and P. Colet, *Stochastic Numerical Methods: An Introduction for Students and Scientists* (Wiley-VCH, Weinheim, 2014).

[36] M. Assaf and B. Meerson, Phys. Rev. Lett. **97**, 200602 (2006).

[37] M. Assaf and B. Meerson, Phys. Rev. E **75**, 031122 (2007).

[38] A. Nitzan, P. Ortoleva, J. Deutch, and J. Ross, J. Chem. Phys. **61**, 1056 (1974).

[39] D. T. Gillespie, J. Stat. Phys. **16**, 311 (1977).

[40] C. R. Doering, K. V. Sargsyan, and L. M. Sander, Multiscale Model. Simul. **3**, 283 (2005).

[41] I. Nåsell, *Extinction and Quasi-Stationarity in the Stochastic Logistic SIS Model*, Lecture Notes in Mathematics Vol. 2022 (Springer, Heidelberg, 2011).

[42] V. Elgart and A. Kamenev, Phys. Rev. E **70**, 041106 (2004).

[43] P. Stephens, W. Sutherland, and R. Freckleton, Oikos **87**, 185 (1999).

[44] M. Assaf, B. Meerson, and P. V. Sasorov, J. Stat. Mech. (2010) P07018.

[45] M. I. Dykman, E. Mori, J. Ross, and P. M. Hunt, J. Chem. Phys. **100**, 5735 (1994).

[46] D. A. Kessler and N. M. Shnerb, J. Stat. Phys. **127**, 861 (2007).

[47] B. Meerson and P. V. Sasorov, Phys. Rev. E **78**, 060103(R) (2008).

[48] C. Escudero and A. Kamenev, Phys. Rev. E **79**, 041149 (2009).

[49] H. Takayasu and A. Y. Tretyakov, Phys. Rev. Lett. **68**, 3060 (1992).

[50] I. Jensen, Phys. Rev. Lett. **70**, 1465 (1993).

[51] I. Jensen, Phys. Rev. E **47**, R1 (1993).

[52] D. Zhong and D. ben-Avraham, Phys. Lett. A **209**, 333 (1995).

[53] J. Cardy and U. C. Täuber, Phys. Rev. Lett. **77**, 4780 (1996).

[54] G. T. Barkema and E. Carlon, Phys. Rev. E **68**, 036113 (2003).

[55] T. M. Liggett, *Interacting Particle Systems* (Springer, Berlin, 2005).

[56] H. Hinrichsen, Adv. Phys. **49**, 815 (2000).

[57] D. ben-Avraham, F. Leyvraz, and S. Redner, Phys. Rev. E **50**, 1843 (1994).